International Conference
ENGINEERING MECHANICS 2010
Svratka, Czech Republic, May 10 – 13, 2010

MESHLESS LOCAL INTEGRAL EQUATION METHOD FOR LAMINATED PLATES

J. Sládek[1], V. Sládek[1], P. Staňák[1], Ch. Zhang[2]

Summary: *Analysis of laminated plates under static and transient dynamic loading is presented by the meshless local Petrov-Galerkin (MLPG) method. Reissner-Mindlin theory is used to describe the governing equations of the plate bending problem. Expressions for the bending moment and shear force are obtained by integration through the laminated plate considering constitutive equations in each lamina. A weak formulation for the set of governing equations with Heaviside step function as the test function is transformed to local integral equations on small local subdomains. The meshless approximation based on the Moving-Least-Squares (MLS) method is employed to obtain a system of ordinary differential equations of the second order for certain nodal unknowns. Houbolt finite-difference scheme is used to solve them as a time-stepping method.*

1. Introduction

Advances in all branches of engineering require structural and construction materials to fulfill higher and higher requirements depending on various operational conditions. Laminated composite plates are widely applied in engineering structures because their properties can be tailored to satisfy those high-performance requirements. Much previous research works have been done for static and dynamic analysis of isotropic thin plates. Previous research results show that the transverse shear effects are more significant for orthotropic plates than for isotropic ones (Wang and Schweizerhof, 1996). It is well known that the classical thin plate theory of Kirchhoff gives rise to certain non-physical simplifications mainly related to the omission of the shear deformation and the rotary inertia, which becomes more significant for increasing thickness of the plate. The Reissner(1946), Mindlin(1951) plate bending theory and higher order shear theories (Reddy, 1997) are widely accepted and applied plate problems. Pagano (1969) obtained analytical solutions for orthotropic simply supported laminates. This benchmark solution has been used to validate new or improved plate theories and finite element formulations (Murakami, 1986). Three-dimensional deformations of multilayered, linear elastic, anisotropic rectangular plates are analyzed by Vel and Batra (1999). They also modelled quasi-static thermoelastic deformations of laminated anisotropic thick plates (Vel and Batra, 2001).

The solution of the boundary or initial boundary value problems for laminated anisotropic plates requires advanced numerical methods due to the high mathematical complexity. Beside

[1] Prof. Ing. Ján Sládek, DrSc., Prof. RNDr. Vladimír Sládek, DrSc., Ing. Peter Staňák: Institute of Construction and Architecture, Slovak Academy of Sciences; Dúbravská cesta 9; 845 03 Bratislava; e-mail: sladek@savba.sk
[2] Prof. Dr.-Ing. habil. Chuanzeng Zhang: Department of Civil Engineering, University of Siegen, Paul-Bonatz-Str. 9-11, D-57068 Siegen, Germany

the well established finite element method (FEM), the boundary element method (BEM) provides an efficient and popular alternative to the FEM. The conventional BEM is accurate and efficient for many engineering problems. However, it requires the availability of the fundamental solutions or Green's functions to the governing partial differential equations (PDE). The material anisotropy increases the number of elastic constants in Hooke´s law, and hence makes the construction of the fundamental solutions cumbersome. The elimination of shear locking in thin walled structures by FEM is difficult and the developed techniques are less accurate. Meshless methods for solving PDE in physics and engineering are a powerful new alternative to the traditional mesh-based techniques. Focusing only on nodes or points instead of elements used in the conventional FEM or BEM, meshless approaches have certain advantages. The moving least-square (MLS) approximation ensures C^1 continuity which satisfies the Kirchhoff hypotheses. One of the most rapidly developed meshfree methods is the Meshless Local Petrov-Galerkin (MLPG) method. The MLPG method has attracted much attention during the past decade (Atluri, 2004) for many problems of continuum mechanics.

In the present paper we will present for the first time a meshless method based on the local Petrov-Galerkin weak-form to solve dynamic problems for laminate plate bending described by the Reissner-Mindlin theory. The bending moment and the shear force expressions are obtained by integration through the laminate plate for the considered constitutive equations in each lamina. The Reissner-Mindlin governing equations of motion are subsequently solved for an elastodynamic plate bending problem. The Reissner-Mindlin theory reduces the original three-dimensional (3-D) thick plate problem to a 2-D problem. In our meshless method, nodal points are randomly distributed over the mean surface of the considered plate. Each node is the center of a circle surrounding this node. Similar approach has been successfully applied to a thin Kirchhoff plate (Sladek et al., 2002) where the governing equation is decomposed into two partial differential equations (PDEs) of the second order. Long and Atluri (2002) applied the meshless local Petrov Galerkin method to solve the bending problem of a thin plate. The MLPG method has been also applied to Reissner-Mindlin plates and shells under dynamic load by Sladek et al. (2007).

Here the weak-form on small subdomains with a Heaviside step function as the test functions is applied to derive local integral equations. Applying the Gauss divergence theorem to the weak-form, the local boundary-domain integral equations are derived. After performing the spatial MLS approximation, a system of ordinary differential equations for certain nodal unknowns is obtained. Then, the system of the ordinary differential equations of the second order resulting from the equations of motion is solved by the Houbolt finite-difference scheme (Houbolt, 1950) as a time-stepping method. Numerical examples are presented and discussed to show the accuracy and the efficiency of the present method.

2. Local integral equations for laminate plate theory

The classical laminate plate theory is an extension of the classical plate theory to composite laminates. Let us consider a plate of total thickness h composed of N orthotropic layers with the mean surface occupying the domain Ω in the plane (x_1, x_2). The $x_3 \equiv z$ axis is perpendicular to the midplane (Fig.1). The k-th layer is located between the points $z = z_k$ and $z = z_{k+1}$ in the thickness direction.

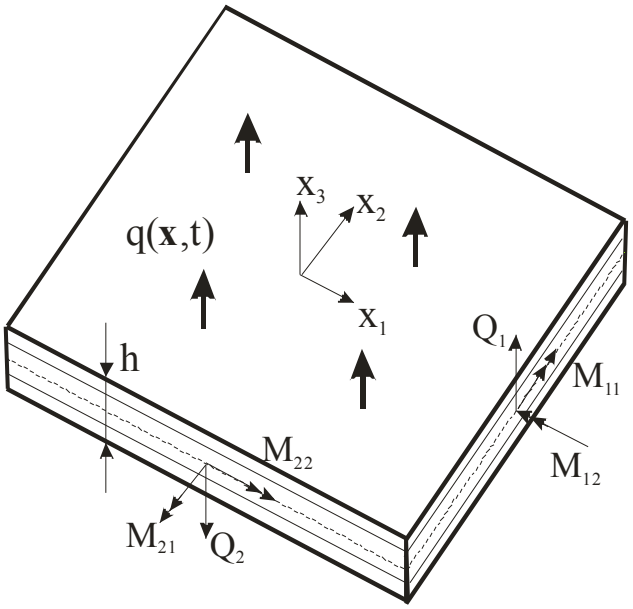

a)

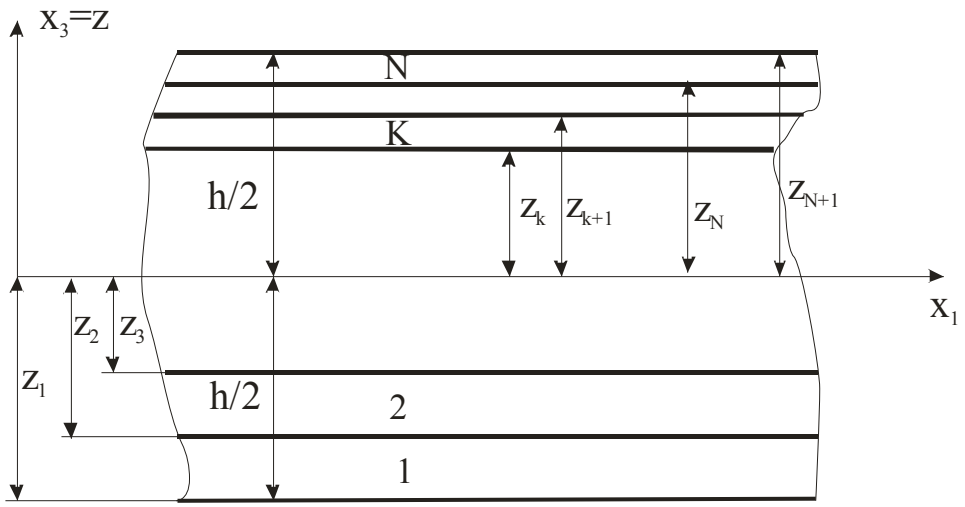

b)

Fig. 1 Laminated plate: a) sign convention of bending moments and forces, b) layer numbering for a general laminated plate

The Reissner-Mindlin plate bending theory (Reissner, 1946; Mindlin, 1951) is used to describe the plate deformation. The transverse shear strains are represented as constant throughout the plate thickness and some correction coefficients are required for computation of transverse shear forces in that theory. Then, the spatial displacement field in time τ, due to transverse loading and expressed in terms of displacement components u_1, u_2, and u_3, has the following form (Reddy, 1997)

$$u_1(\mathbf{x}, x_3, \tau) = x_3 w_1(\mathbf{x}, \tau)$$

$$u_2(\mathbf{x}, x_3, \tau) = x_3 w_2(\mathbf{x}, \tau)$$

$$u_3(\mathbf{x}, \tau) = w_3(\mathbf{x}, \tau) \tag{1}$$

where $w_\alpha(x_1, x_2, \tau)$ and $w_3(x_1, x_2, \tau)$ represent the rotations around the in-plane axes and the out-of-plane deflection, respectively (Fig. 1).

Linear strains are given by

$$\varepsilon_{11}(\mathbf{x}, x_3, \tau) = x_3 w_{1,1}(\mathbf{x}, \tau)$$
$$\varepsilon_{22}(\mathbf{x}, x_3, \tau) = x_3 w_{2,2}(\mathbf{x}, \tau)$$
$$\varepsilon_{12}(\mathbf{x}, x_3, \tau) = x_3 (w_{1,2}(\mathbf{x}, \tau) + w_{2,1}(\mathbf{x}, \tau))/2$$
$$\varepsilon_{13}(\mathbf{x}, \tau) = (w_1(\mathbf{x}, \tau) + w_{3,1}(\mathbf{x}, \tau))/2$$

$$\varepsilon_{23}(\mathbf{x}, \tau) = (w_2(\mathbf{x}, \tau) + w_{3,2}(\mathbf{x}, \tau))/2 \tag{2}$$

In the case of orthotropic materials for the k-th lamina, the relation between the stress σ_{ij} and the strain ε_{ij} is described by the constitutive equations for the stress tensor

$$\sigma_{ij}^{(k)}(\mathbf{x}, x_3, \tau) = c_{ijml}^{(k)} \varepsilon_{ml}(\mathbf{x}, x_3, \tau) \tag{3}$$

where the material stiffness coefficients $c_{ijml}^{(k)}$ are assumed homogeneous for the k-th lamina.

For plane problems the constitutive equation (3) is frequently written in terms of the second-order tensor of elastic constants (Lekhnitskii, 1963). The constitutive equation for orthotropic materials and plane stress problem has the following form

$$\begin{bmatrix} \sigma_{11} \\ \sigma_{22} \\ \sigma_{12} \\ \sigma_{13} \\ \sigma_{23} \end{bmatrix}^{(k)} = \mathbf{G}^{(k)}(\mathbf{x}) \begin{bmatrix} \varepsilon_{11} \\ \varepsilon_{22} \\ 2\varepsilon_{12} \\ 2\varepsilon_{13} \\ 2\varepsilon_{23} \end{bmatrix} \tag{4}$$

where

$$\mathbf{G}^{(k)}(\mathbf{x}) = \begin{bmatrix} E_1^{(k)}/e^{(k)} & E_1^{(k)}\nu_{21}^{(k)}/e^{(k)} & 0 & 0 & 0 \\ E_2^{(k)}\nu_{12}^{(k)}/e^{(k)} & E_2^{(k)}/e^{(k)} & 0 & 0 & 0 \\ 0 & 0 & G_{12}^{(k)} & 0 & 0 \\ 0 & 0 & 0 & G_{13}^{(k)} & 0 \\ 0 & 0 & 0 & 0 & G_{23}^{(k)} \end{bmatrix} \quad \text{with} \quad e^{(k)} = 1 - \nu_{12}^{(k)}\nu_{21}^{(k)}$$

$E_\alpha^{(k)}$ are the Young´s moduli refering to the axes x_α, $\alpha = 1, 2$, $G_{12}^{(k)}$, $G_{13}^{(k)}$ and $G_{23}^{(k)}$ are shear moduli, ν_{12} and ν_{21} are Poisson´s ratios.

Despite the stress discontinuities, one can define the integral quantities such as the bending moments $M_{\alpha\beta}$ and the shear forces Q_α with $\kappa = 5/6$ from the Reissner plate theory as

$$\begin{bmatrix} M_{11} \\ M_{22} \\ M_{12} \end{bmatrix} = \int_{-h/2}^{h/2} \begin{bmatrix} \sigma_{11} \\ \sigma_{22} \\ \sigma_{12} \end{bmatrix} x_3 dx_3 = \sum_{k=1}^{N} \int_{z_k}^{z_{k+1}} \begin{bmatrix} \sigma_{11} \\ \sigma_{22} \\ \sigma_{12} \end{bmatrix}^{(k)} x_3 dx_3$$

$$\begin{bmatrix} Q_1 \\ Q_2 \end{bmatrix} = \kappa \int_{-h/2}^{h/2} \begin{bmatrix} \sigma_{13} \\ \sigma_{23} \end{bmatrix} dx_3 = \kappa \sum_{k=1}^{N} \int_{z_k}^{z_{k+1}} \begin{bmatrix} \sigma_{13} \\ \sigma_{23} \end{bmatrix}^{(k)} dx_3 \tag{5}$$

Substituting equations (4) and (2) into moment and force resultants (5) allows the expression of the bending moments $M_{\alpha\beta}$ and shear forces Q_α for α,β=1,2, in terms of rotations and lateral displacements of the orthotropic plate. In the case of considered layer-wise material properties through the plate thickness, one obtains

$$M_{\alpha\beta} = D_{\alpha\beta}\left(w_{\alpha,\beta} + w_{\beta,\alpha}\right) + C_{\alpha\beta} w_{\gamma,\gamma}$$

$$Q_\alpha = C_\alpha \left(w_\alpha + w_{3,\alpha}\right) \tag{6}$$

where repeated indices α, β do not imply summation and the material parameters $D_{\alpha\beta}$ and $C_{\alpha\beta}$ are given as

$$2D_{11} = \int_{-h/2}^{h/2} z^2 E_1(z) \frac{1-\nu_{21}}{e} dz = \sum_{k=1}^{N} \int_{z_k}^{z_{k+1}} E_1^{(k)} \frac{1-\nu_{21}^{(k)}}{e^{(k)}} z^2 dz = \sum_{k=1}^{N} E_1^{(k)} \frac{1-\nu_{21}^{(k)}}{e^{(k)}} \frac{1}{3}\left(z_{k+1}^3 - z_k^3\right),$$

$$2D_{22} = \int_{-h/2}^{h/2} z^2 E_2(z) \frac{1-\nu_{12}}{e} dz = \sum_{k=1}^{N} E_2^{(k)} \frac{1-\nu_{12}^{(k)}}{e^{(k)}} \frac{1}{3}\left(z_{k+1}^3 - z_k^3\right),$$

$$D_{12} = \int_{-h/2}^{h/2} z^2 G_{12}(z) dz = \sum_{k=1}^{N} G_{12}^{(k)} \frac{1}{3}\left(z_{k+1}^3 - z_k^3\right),$$

$$C_{11} = \int_{-h/2}^{h/2} z^2 E_1(z) \frac{\nu_{21}}{e} dz = \sum_{k=1}^{N} E_1^{(k)} \frac{\nu_{21}^{(k)}}{e^{(k)}} \frac{1}{3}\left(z_{k+1}^3 - z_k^3\right),$$

$$C_{22} = \int_{-h/2}^{h/2} z^2 E_2(z) \frac{\nu_{12}}{e} dz = \sum_{k=1}^{N} E_2^{(k)} \frac{\nu_{12}^{(k)}}{e^{(k)}} \frac{1}{3}\left(z_{k+1}^3 - z_k^3\right), \quad C_{12} = C_{21} = 0,$$

$$C_\alpha = \kappa \int_{-h/2}^{h/2} G_{\alpha 3}(z) dz = \kappa \sum_{k=1}^{N} G_{\alpha 3}^{(k)} \left(z_{k+1} - z_k\right). \tag{7}$$

For a homogeneous plate, equations (7) are transformed into a simpler form

$$D_{11} = \frac{D_1}{2}\left(1-\nu_{21}\right), \quad D_{22} = \frac{D_2}{2}\left(1-\nu_{12}\right), \quad D_{12} = D_{21} = \frac{\bar{G}_{12} h^3}{12}, \quad D_\alpha = \frac{E_\alpha h^3}{12e},$$

$$C_{11} = D_1 \nu_{21}, \quad C_{22} = D_2 \nu_{12}, \quad C_{12} = C_{21} = 0,$$

$$D_1 \nu_{21} = D_2 \nu_{12}, \quad C_\alpha = \kappa h G_{\alpha 3} \tag{8}$$

Assuming the mass density to be homogeneous within each lamina and using the Reissner's linear theory of thick plates (Reissner, 1946), the equations of motion may be written as

$$M_{\alpha\beta,\beta}(\mathbf{x},\tau) - Q_\alpha(\mathbf{x},\tau) = I_M \ddot{w}_\alpha(\mathbf{x},\tau) \tag{9}$$

$$Q_{\alpha,\alpha}(\mathbf{x},\tau)+q(\mathbf{x},\tau)=I_Q\ddot{w}_3(\mathbf{x},\tau),\quad \mathbf{x}\in\Omega \tag{10}$$

where

$$I_M=\int_{-h/2}^{h/2}z^2\rho(z)dz=\sum_{k=1}^{N}\int_{z_k}^{z_{k+1}}\rho^{(k)}z^2dz=\sum_{k=1}^{N}\rho^{(k)}\frac{1}{3}\left(z_{k+1}^3-z_k^3\right)$$

$$I_Q=\int_{-h/2}^{h/2}\rho(z)dz=\sum_{k=1}^{N}\int_{z_k}^{z_{k+1}}\rho^{(k)}dz=\sum_{k=1}^{N}\rho^{(k)}\left(z_{k+1}-z_k\right)$$

are global inertial characteristics of the laminated plate. The Greek indices vary from 1 to 2. If the mass density is constant throughout the plate thickness, we obtain

$$I_M=\frac{\rho h^3}{12},\quad I_Q=\rho h.$$

The dots over a quantity indicate differentiations with respect to time τ.

Instead of writing the global weak-form for the above governing equations, the MLPG methods construct the weak-form over local subdomains such as Ω_s, which is a small region taken for each node inside the global domain (Atluri, 2004). The local subdomains overlap each other and cover the whole global domain Ω as seen in Fig. 2. The local subdomains could be of any geometrical shape and size. In the current paper, the local subdomains are taken to be of circular shape. The local weak-form of the governing equations (9) and (10) for $\mathbf{x}^i\in\Omega_s^i$ can be written as

$$\int_{\Omega_s^i}\left[M_{\alpha\beta,\beta}(\mathbf{x},\tau)-Q_\alpha(\mathbf{x},\tau)-I_M\ddot{w}_\alpha(\mathbf{x},\tau)\right]w_{\alpha\gamma}^*(\mathbf{x})d\Omega=0 \tag{11}$$

$$\int_{\Omega_s^i}\left[Q_{\alpha,\alpha}(\mathbf{x},\tau)+q(\mathbf{x},\tau)-I_Q\ddot{w}_3(\mathbf{x},\tau)\right]w_3^*(\mathbf{x})d\Omega=0 \tag{12}$$

where $w_{\alpha\gamma}^*(\mathbf{x})$ and $w^*(\mathbf{x})$ are weight or test functions.

Applying the Gauss divergence theorem to Eqs. (11) and (12) one obtains

$$\int_{\partial\Omega_s^i}M_\alpha(\mathbf{x},\tau)w_{\alpha\gamma}^*(\mathbf{x})d\Gamma-\int_{\Omega_s^i}M_{\alpha\beta}(\mathbf{x},\tau)w_{\alpha\gamma,\beta}^*(\mathbf{x})d\Omega-\int_{\Omega_s^i}Q_\alpha(\mathbf{x},\tau)w_{\alpha\gamma}^*(\mathbf{x})d\Omega-$$

$$-\int_{\Omega_s^i}I_M\ddot{w}_\alpha(\mathbf{x},\tau)w_{\alpha\gamma}^*(\mathbf{x})d\Omega=0 \tag{13}$$

$$\int_{\partial\Omega_s^i}Q_\alpha(\mathbf{x},\tau)n_\alpha(\mathbf{x})w^*(\mathbf{x})d\Gamma-\int_{\Omega_s^i}Q_\alpha(\mathbf{x},\tau)w_{,\alpha}^*(\mathbf{x})d\Omega-\int_{\Omega_s^i}I_Q\ddot{w}_3(\mathbf{x},\tau)w^*(\mathbf{x})d\Omega+$$

$$+\int_{\Omega_s^i}q(\mathbf{x},\tau)w^*(\mathbf{x})d\Omega=0 \tag{14}$$

where $\partial\Omega_s^i$ is the boundary of the local subdomain and $M_\alpha(\mathbf{x},\tau)=M_{\alpha\beta}(\mathbf{x},\tau)n_\beta(\mathbf{x})$ is the normal bending moment, n_α is the unit outward normal vector to the boundary $\partial\Omega_s^i$. The local weak-forms (13) and (14) are the starting point for deriving local boundary integral equations on the basis of appropriate test functions. Unit step functions are chosen for the test functions $w_{\alpha\gamma}^*(\mathbf{x})$ and $w^*(\mathbf{x})$ in each subdomain

$$w^*_{\alpha\gamma}(\mathbf{x}) = \begin{cases} \delta_{\alpha\gamma} & \text{at } \mathbf{x} \in (\Omega_s \cup \partial\Omega_s) \\ 0 & \text{at } \mathbf{x} \notin (\Omega_s \cup \partial\Omega_s) \end{cases}, \quad w^*(\mathbf{x}) = \begin{cases} 1 & \text{at } \mathbf{x} \in (\Omega_s \cup \partial\Omega_s) \\ 0 & \text{at } \mathbf{x} \notin (\Omega_s \cup \partial\Omega_s) \end{cases} \tag{15}$$

Then, the local weak-forms (13, 14) are transformed into the following local integral equations

$$\int_{\partial\Omega_s^i} M_\alpha(\mathbf{x},\tau)d\Gamma - \int_{\Omega_s^i} Q_\alpha(\mathbf{x},\tau)d\Omega - \int_{\Omega_s^i} I_M \ddot{w}_\alpha(\mathbf{x},\tau)d\Omega = 0 \tag{16}$$

$$\int_{\partial\Omega_s^i} Q_\alpha(\mathbf{x},\tau)n_\alpha(\mathbf{x})d\Gamma - \int_{\Omega_s^i} I_Q \ddot{w}_3(\mathbf{x},\tau)d\Omega + \int_{\Omega_s^i} q(\mathbf{x},\tau)d\Omega = 0 \tag{17}$$

In the above local integral equations, the trial functions $w_\alpha(\mathbf{x},\tau)$, related to rotations, and $w_3(\mathbf{x},\tau)$, related to transversal displacements, are chosen as the moving least-squares (MLS) interpolation over a number of nodes randomly spread within the domain of influence as described in the following Section 3. Let us notice, that the local subdomain is defined as the support of the test function on which the integration is performed and the domain of influence is defined as a region where the test function is not zero and all nodes lying inside are considered for interpolation.

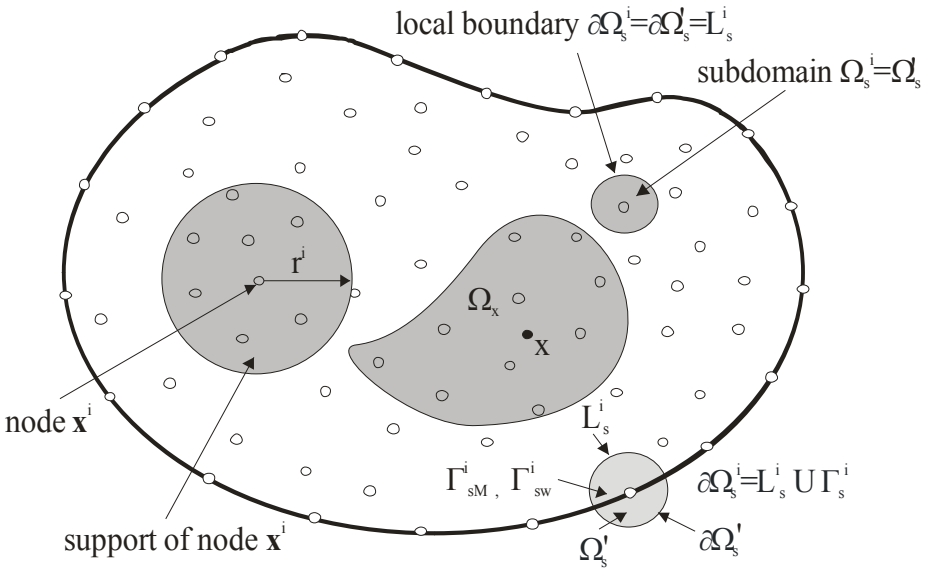

Fig. 2 Local boundaries for weak formulation, the domain Ω_x for MLS approximation of the trial function, and support area of weight function around node $\mathbf{x}^i$

3. Numerical solution

In general, a meshless method uses a local interpolation to represent the trial function with the values (or the fictitious values) of the unknown variable at some randomly located nodes. The

moving least-squares (MLS) approximation (Lancaster and Salkauskas, 1981; Atluri 2004) used in the present analysis may be considered as one of such schemes. Let us consider a sub-domain Ω_x of the problem domain Ω in the neighbourhood of a point **x** for the definition of the MLS approximation of the trial function around ***x*** (Fig. 2). To approximate the distribution of the generalized displacements (rotations and deflection) in Ω_x over a number of randomly located nodes $\left\{\mathbf{x}^a\right\}$, $a = 1,2,...n$, the MLS approximant $w_i^h(\mathbf{x},\tau)$ of $w_i(\mathbf{x},\tau)$ is defined by Atluri (2004) as

$$\mathbf{w}^h(\mathbf{x},\tau) = \mathbf{\Phi}^T(\mathbf{x}) \cdot \hat{\mathbf{w}}(\tau) = \sum_{a=1}^{n} \phi^a(\mathbf{x}) \hat{\mathbf{w}}^a(\tau) \tag{18}$$

where $\mathbf{w}^h = \left[w_1^h, w_2^h, w_3^h \right]^T$ and $\hat{\mathbf{w}}^a(\tau)$ are the fictitious nodal values, but not the nodal values of the unknown trial function $\mathbf{w}^h(\mathbf{x},\tau)$, in general. Recall that *n* is the number of nodes in Ω_x.

In eq. (18), $\phi^a(\mathbf{x})$ is usually referred to as the shape function of the MLS approximation corresponding to the nodal point $\mathbf{x}^a$. The support domain of the nodal point $\mathbf{x}^a$ is usually taken to be a circle of the radius r^a centred at $\mathbf{x}^a$ (see Fig. 2). There are various weight functions $v^a(\mathbf{x})$ available for obtaining $\phi^a(\mathbf{x})$ as shown by Atluri (2004), in this work a 4th-order spline-type weight function is applied. In practical applications, $v^a(\mathbf{x})$ is often chosen in such a way that it is non-zero over the support of the nodal point $\mathbf{x}^a$. With such weigh function, the C^1-continuity of the weight function is ensured over the entire domain; therefore the continuity condition of the bending moments and the shear forces is satisfied. The size of the support r^a should be large enough to cover a sufficient number of nodes in the domain of definition to ensure the regularity of evaluated matrices. The value of *n* is determined by the number of nodes lying in the support domain with radius r^a.

The directional derivatives of $\mathbf{w}(\mathbf{x},\tau)$ are approximated in terms of same nodal values as

$$\mathbf{w}_{,k}(\mathbf{x},\tau) = \sum_{a=1}^{n} \hat{\mathbf{w}}^a(\tau) \phi_{,k}^a(\mathbf{x}) \tag{19}$$

Substituting the approximation (19) into the definition of the normal bending (6), one obtains for $\mathbf{M}(\mathbf{x},\tau) = \left[M_1(\mathbf{x},\tau),\ M_2(\mathbf{x},\tau) \right]^T$ expression in form

$$\mathbf{M}(\mathbf{x},\tau) = \mathbf{N}_1 \sum_{a=1}^{n} \mathbf{B}_1^a(\mathbf{x}) \mathbf{w}^{*a}(\tau) \ + \mathbf{N}_2 \sum_{a=1}^{n} \mathbf{B}_2^a(\mathbf{x}) \mathbf{w}^{*a}(\tau) \ = \mathbf{N}_\alpha(\mathbf{x}) \sum_{a=1}^{n} \mathbf{B}_\alpha^a(\mathbf{x}) \mathbf{w}^{*a}(\tau) \tag{20}$$

where the vector $\mathbf{w}^{*a}(\tau)$ is defined as a column vector $\mathbf{w}^{*a}(\tau) = \left[\hat{w}_1^a(\tau),\ \hat{w}_2^a(\tau) \right]^T$, the matrices $\mathbf{N}_\alpha(\mathbf{x})$ are related to the normal vector **n(x)** on $\partial\Omega_s$, and the matrices $\mathbf{B}_\alpha^a$ are represented by the gradients of the shape functions $\phi^a{}_{,1}$ and $\phi^a{}_{,2}$ and parameters $D_{\alpha\beta}$ (Sladek et al., 2007). The influence of the material properties for composite laminas is incorporated in $C_{\alpha\beta}$ and $D_{\alpha\beta}$ defined in equations (7).

Similarly one can obtain the approximation for the shear forces

$$\mathbf{Q}(\mathbf{x},\tau)=\mathbf{C}(\mathbf{x})\sum_{a=1}^{n}\left[\phi^{a}(\mathbf{x})\mathbf{w}^{*a}(\tau)+\mathbf{F}^{a}(\mathbf{x})\hat{w}_{3}^{a}(\tau)\right] \tag{21}$$

where $\mathbf{Q}(\mathbf{x},\tau)=\left[Q_1(\mathbf{x},\tau),\ Q_2(\mathbf{x},\tau)\right]^T$ and $\mathbf{F}^{a}(\mathbf{x})=\left[\phi_{,1}^{a}\quad \phi_{,2}^{a}\right]^T$.

Then, insertion of the MLS-discretized force fields (20) and (21) into the local integral equations (16) and (17) yields the discretized local integral equations (LIEs)

$$\sum_{a=1}^{n}\left[\int_{L_s^i+\Gamma_{sw}^i}\mathbf{N}_{\alpha}(\mathbf{x})\mathbf{B}_{\alpha}^{a}(\mathbf{x})d\Gamma-\int_{\Omega_s^i}\mathbf{C}(\mathbf{x})\phi^{a}(\mathbf{x})d\Omega\right]\mathbf{w}^{*a}(\tau)\ -\sum_{a=1}^{n}I_M\ddot{\mathbf{w}}^{*a}(\tau)\int_{\Omega_s^i}\phi^{a}(\mathbf{x})d\Omega-$$

$$-\sum_{a=1}^{n}\hat{w}_{3}^{a}(\tau)\int_{\Omega_s^i}\mathbf{C}(\mathbf{x})\mathbf{F}^{a}(\mathbf{x})d\Omega=-\int_{\Gamma_{sM}^i}\tilde{\mathbf{M}}(\mathbf{x},\tau)d\Gamma \tag{22}$$

$$\sum_{a=1}^{n}\left(\int_{\partial\Omega_s^i}\mathbf{C}_n(\mathbf{x})\phi^{a}(\mathbf{x})d\Gamma\right)\mathbf{w}^{*a}(s)+\sum_{a=1}^{n}\hat{w}_{3}^{a}(s)\left(\int_{\partial\Omega_s^i}\mathbf{C}_n(\mathbf{x})\mathbf{F}^{a}(\mathbf{x})d\Gamma\right)\ =$$

$$-I_Q\sum_{a=1}^{n}\ddot{\hat{w}}_{3}^{a}(\tau)\left(\int_{\Omega_s^i}\phi^{a}(\mathbf{x})d\Omega\right)\ =-\int_{\Omega_s^i}q(\mathbf{x},\tau)d\Omega \tag{23}$$

where $\mathbf{C}_n(\mathbf{x})=\left(n_1,\ n_2\right)\mathbf{C}(\mathbf{x})=\left(C_1n_1,\ C_2n_2\right)$ and $\mathbf{C}(\mathbf{x})$ represents material properties.

Equations (22) and (23) are considered on the subdomains adjacent to the interior nodes $\mathbf{x}^i$ as well as to the boundary nodes on Γ_{sM}^i . For the source point $\mathbf{x}^i$ located on the global boundary Γ the boundary of the subdomain $\partial\Omega_s^i$ is decomposed into L_s^i and Γ_{sM}^i (part of the global boundary with prescribed bending moment) according to Fig. 2.

It should be noted here that there are neither Lagrange multipliers nor penalty parameters introduced into the local weak forms (11) and (12) because the essential boundary conditions on Γ_{sw}^i (part of the global boundary with prescribed rotations or displacements) can be imposed directly, using the interpolation approximation (18)

$$\sum_{a=1}^{n}\phi^{a}(\mathbf{x}^i)\hat{\mathbf{w}}^{a}(\tau)=\tilde{\mathbf{w}}(\mathbf{x}^i,\tau)\ \text{ for }\ \mathbf{x}^i\in\Gamma_{sw}^i \tag{24}$$

where $\tilde{\boldsymbol{w}}(\mathbf{x}^i,\tau)$ is the generalized displacement vector prescribed on the boundary Γ_{sw}^i.

Collecting the discretized local boundary-domain integral equations together with the discretized boundary conditions for the generalized displacements, one obtains a complete system of ordinary differential equations and it can be rearranged in such a way that all known quantities are on the r.h.s. Thus, in matrix form the system becomes

$$\mathbf{A}\ddot{\mathbf{x}}+\mathbf{C}\mathbf{x}=\mathbf{Y} \tag{25}$$

Recall that the system matrix has a block structure. There are many time integration procedures for the solution of this system of ordinary differential equations. In the present work, the Houbolt method is applied. In the Houbolt finite- difference scheme (Houbolt, 1950), the "acceleration" $\left(\ddot{\mathbf{u}}=\ddot{\mathbf{x}}\right)$ is expressed as

$$\ddot{\mathbf{x}}_{\tau+\Delta\tau} = \frac{2\mathbf{x}_{\tau+\Delta\tau} - 5\mathbf{x}_{\tau} + 4\mathbf{x}_{\tau-\Delta\tau} - \mathbf{x}_{\tau-2\Delta\tau}}{\Delta\tau^2} \tag{26}$$

where $\Delta\tau$ is the time step. Substituting eq. (26) into eq. (25), we get the following system of algebraic equations for the unknowns $\mathbf{x}_{\tau+\Delta\tau}$

$$\left[\frac{2}{\Delta\tau^2}\mathbf{A} + \mathbf{C}\right]\mathbf{x}_{\tau+\Delta\tau} = \frac{1}{\Delta\tau^2}5\mathbf{A}\mathbf{x}_{\tau} + \mathbf{A}\frac{1}{\Delta\tau^2}\left\{-4\mathbf{x}_{\tau-\Delta\tau} + \mathbf{x}_{\tau-2\Delta\tau}\right\} + \mathbf{Y} \tag{27}$$

The value of the time step has to be appropriately selected with respect to material parameters (wave velocities) and time dependence of the boundary conditions.

4. Numerical examples

4.1 Clamped three-ply square plate

Consider a clamped square plate with a side-length $a = 0.254m$ and the plate thicknesses $h = 0.0127m$. The plate is subjected to a uniformly distributed static load. Homogeneous material properties are considered at first to test accuracy of the present computational method. Then orthotropic properties are considered. The following material parameters are used in numerical analysis: Young's moduli $E_2 = 0.6895 \cdot 10^{10}\ \mathrm{N/m^2}$, $E_1 = 2E_2$, Poisson's ratios $\nu_{21} = 0.15$, $\nu_{12} = 0.3$ and mass density $\rho = 5.0 \times 10^3\ \mathrm{kg/m^3}$. Shear moduli used correspond to Young's modulus E_2, namely, $G_{12} = G_{13} = G_{23} = E_2 / 2(1+\nu_{12})$.

In our numerical calculations, 441 nodes with a regular distribution were used for the approximation of the rotations and the deflection. The origin of the coordinate system is located at the center of the plate (Fig. 1a)). The deflection value is normalized by the corresponding central deflection of an isotropic homogeneous plate, considering $E_1 = E_2$, $\nu_{12} = \nu_{21} = 0.3$. For a uniformly distributed load $q_0 = 300\ \mathrm{psi}\,(2.07 \times 10^6\ \mathrm{Nm^{-2}})$ we have $w_3^{iso}(0) = 8.842 \cdot 10^{-3} m$. The numerical results are compared with the results obtained by the FEM-ANSYS code with a very fine mesh of 900 quadrilateral eight-node shell elements for a quarter of the plate.

The clamped three-ply square plate under a static uniform load is analyzed. Geometrical parameters are the same as in the previous homogeneous case. The bottom and top layers have the same thickness $h_1 = h_3 = h/4$. Young`s moduli for both bottom and top layers are the same and they are 5 time larger than ones corresponding to the homogeneous orthotropic plate. The second mid-layer has the same material properties as the homogeneous orthotropic plate analyzed previously. For the numerical modelling we have used again 441 nodes with a regular distribution. The variation of the deflection with the x_1-coordinate at $x_2 = 0$ of the plate is presented in Fig. 3. One can observe that the deflection value is reduced for the laminated orthotropic plate due to the larger flexural rigidity. The variation of the bending moment M_{11} is presented in Fig. 4. Here, the bending moments are normalized by the central bending moment value corresponding to an isotropic homogeneous plate $M_{11}^{iso}(0) = 3064 Nm$. If you compare bending moments for orthotropic homogeneus plate shown in Fig. 4 with re-

sults for orthotropic laminated plate, the results are very similar. It means that considered lamination has vanishing influence on the bending moment variation.

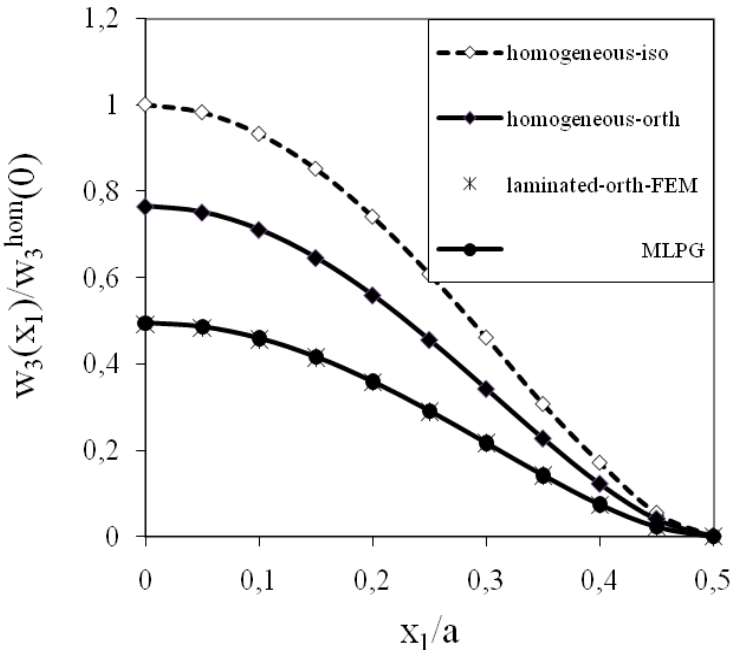

Fig. 3 Variation of deflection with the x_1 -coordinate for a clamped laminated square plate

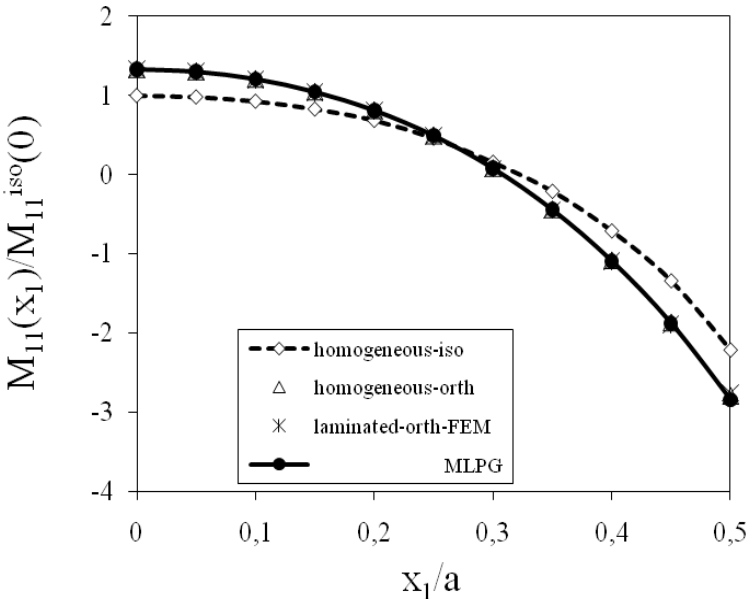

Fig. 4 Variation of bending moment with the x_1 -coordinate for a clamped laminated plate

Clamped orthotropic laminated square plate under an impact load with Heaviside time variation is analyzed too. Geometrical and material parameters are the same as in the previous

static case. Numerical calculations are carried out for a time step $\Delta\tau = 0.357 \cdot 10^{-4} s$. The time variations of the central deflection and the bending moment M_{11} are given in Fig. 5 and Fig. 6, respectively. Both quantities are normalized by their corresponding static values at the center of the isotropic homogeneous plate. Time is normalized by $\tau_0 = a^2 / 4\sqrt{\rho h / D} = 0.3574 \cdot 10^{-2} s$.

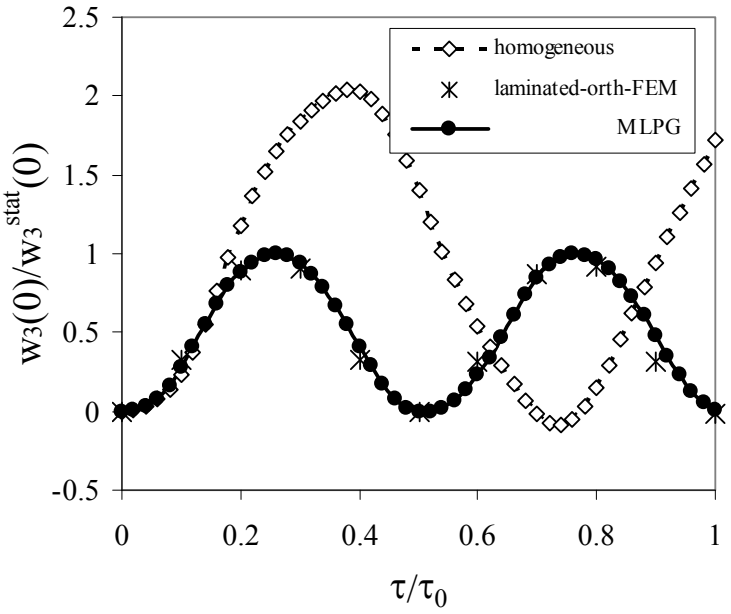

Fig. 5 Time variation of the deflection at the centre of a clamped laminated plate subjected to a suddenly applied load

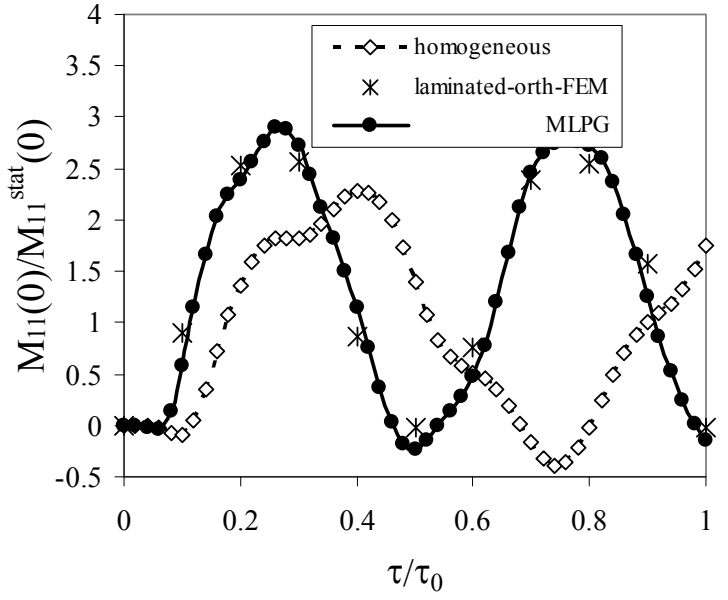

Fig. 6 Time variation of the bending moment at the centre of a clamped laminated plate subjected to a suddenly applied load

The MLPG results are compared with those obtained by FEM-ANSYS computer code. A good agreement of the present results for the deflections and the bending moments at the central point and the FEM results is observed in every figure.

4.2 Simply supported three-ply square plate

A simply supported three-ply square plate under a static uniform load is analyzed. The used geometrical and material parameters are the same as in the previous clamped plate. For the numerical modelling we have used again 441 nodes with a regular distribution. A uniformly distributed load $q_0 = 300$ psi$(2.07\times10^6$ Nm$^{-2})$ is considered here. The deflection value is normalized by the corresponding central deflection of an isotropic homogeneous plate $w_3^{iso}(0) = 0.02829m$. The variation of the deflection with the x_1-coordinate at $x_2 = 0$ of the plate is presented in Fig. 7. One can observe that the deflection value is reduced for the homogeneous orthotropic plate due to the larger flexural rigidity. Higher deflection reduction is seen for laminated orthotropic plate due to further flexural rigidity increase.

The variation of the bending moments M_{11} is shown in Fig. 8. The bending moment at the centre of the plate $M_{11}^{iso}(0) = 6482Nm$ is used as a normalized parameter. The bending moments are enlarged for the orthotropic homogeneous or laminated plates with respect to the moments for isotropic plate. The lamination has vanishing influence on the bending moments. The MLPG results are again compared with those obtained by FEM-ANSYS computer code.

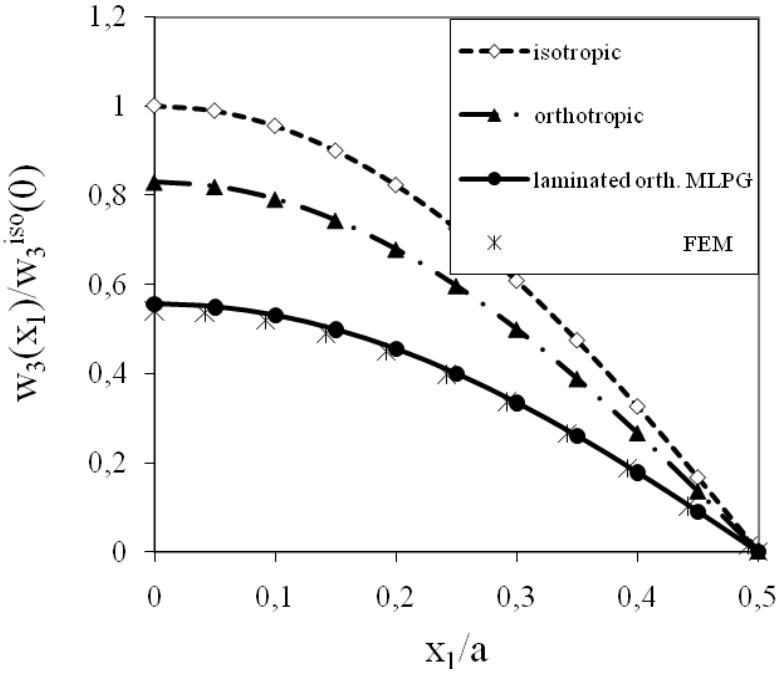

Fig. 7 Variation of the deflection with the x_1 -coordinate for simply supported square plates

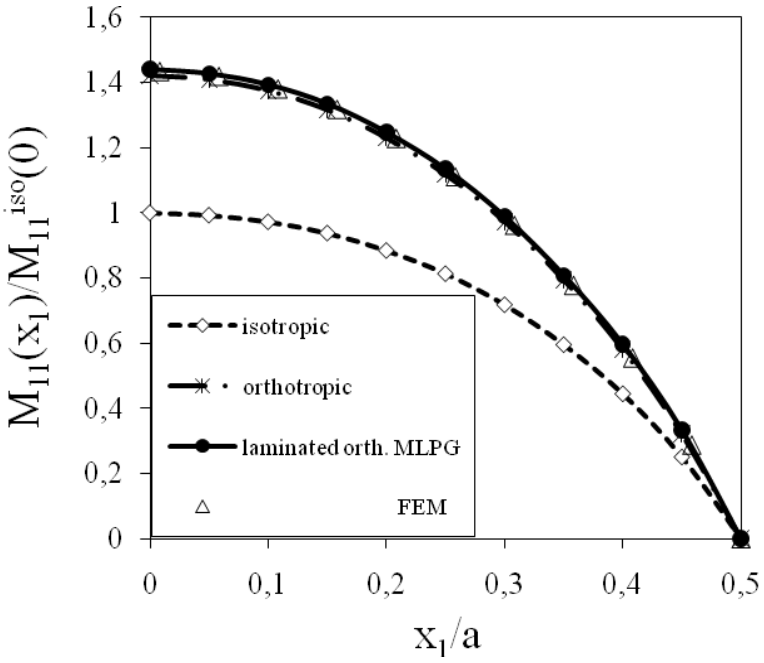

Fig. 8 Variation of the bending moment with the x_1 -coordinate for simply supported square plates

5. Conclusion

A meshless local Petrov-Galerkin method is applied to laminated plates under mechanical loadings. Both stationary and impact loads are considered. The present computational method has no restriction on number of laminae and their material properties. The laminated plate bending problem is described by the Reissner-Mindlin theory. The weak-form on small subdomains with a Heaviside step function as the test functions is applied to derive local integral equations. After performing the spatial MLS approximation, a system of ordinary differential equations for certain nodal unknowns is obtained. Then, the system of the ordinary differential equations of the second order resulting from the equations of motion is solved by the Houbolt finite-difference scheme as a time-stepping method.

The proposed method is a truly meshless method, which requires neither domain elements nor background cells in either the interpolation or the integration. It is demonstrated numerically that the quality of the results obtained by the proposed MLPG method is very good. The degree of the agreement of our numerical results with those obtained by the FEM-ANSYS computer code ranges from good to excellent.

6. Acknowledgement

The authors acknowledge the support by the Slovak Science and Technology Assistance Agency registered under number APVV-0427-07, the Slovak Grant Agency VEGA-2/0039/09, and the German Research Foundation (DFG, Project-No ZH 15/6-3).

7. References

Atluri, S. N. (2004): *The Meshless Method , (MLPG) For Domain & BIE Discretizations*, Tech Science Press.

Houbolt, J.C. (1950): A recurrence matrix solution for the dynamic response of elastic aircraft, *Journal of Aeronautical Sciences*, 17: 371-376.

Lancaster, P.; Salkauskas, T. (1981): Surfaces generated by moving least square methods, *Math. Comput.*, 37: 141-158.

Lekhnitskii, S.G. (1963): *Theory of Elasticity of an Anisotropic Body*. Holden Day.

Long, S.Y.; Atluri, S.N. (2002): A meshless local Petrov Galerkin method for solving the bending problem of a thin plate. *CMES: Computer Modeling in Engineering & Sciences*, 3: 11-51.

Mindlin, R.D. (1951): Influence of rotary inertia and shear on flexural motions of isotropic, elastic plates. *Journal of Applied Mechanics ASME*, 18: 31-38.

Murakami, H. (1986): Laminated composite plate theory with improved in-plane responses. *Journal of Applied Mechanics ASME*, 53: 661-666.

Pagano, N.J. (1969): Exact solutions for composite laminates in cylindrical bending, *Journal of Composite Materials*, 3: 398-411.

Reddy J.N. (1997): *Mechanics of Laminated Composite Plates: Theory and Analysis*. CRC Press, Boca Raton.

Reissner, E. (1946): Stresses and small displacements analysis of shallow shells-II, *Journal Math. Physics*, 25: 279-300.

Sladek, J.; Sladek, V.; Mang, H.A. (2002): Meshless formulations for simply supported and clamped plate problems. *Int. J. Num. Meth. Engn*., 55: 359-375.

Sladek, J.; Sladek, V.; Krivacek, J.; Wen, P.; Zhang, Ch. (2007): Meshless Local Petrov-Galerkin (MLPG) method for Reissner-Mindlin plates under dynamic load. *Computer Meth. Appl. Mech. Engn.*, 196: 2681-2691.

Vel, S.; Batra, R.C. (1999): Analytical solution of rectangular thick plates subjected to arbitrary boundary conditions. *AIAA Journal*, 37: 1464-1473.

Vel, S.; Batra, R.C. (2001): Generalized plane strain thermoelastic deformation of laminated anisotropic thick plates. *International Journal of Solids and Structures*, 38: 1395-1414.

Wang J.; Schweizerhof K. (1996): Study on free vibration of moderately thick orthotropic laminated shallow shells by boundary-domain elements. *Applied Mathematical Modelling,* 20: 579-584.